MOLECULAR AND CELLULAR BIOLOGY, Mar. 2009, p. 1107–1115 Vol. 29, No. 5
0270-7306/09/$08.00+0 doi:10.1128/MCB.01262-08

Regulation of SMN Protein Stability▽†

Barrington G. Burnett,[1]* Eric Muñoz,[1] Animesh Tandon,[1] Deborah Y. Kwon,[1] Charlotte J. Sumner,[2] and Kenneth H. Fischbeck[1]

Neurogenetics Branch, National Institute of Neurological Disorders and Stroke, National Institutes of Health, Bethesda, Maryland,[1] *and Department of Neurology, Johns Hopkins University, Baltimore, Maryland*[2]

Received 8 August 2008/Returned for modification 16 September 2008/Accepted 8 December 2008

Spinal muscular atrophy (SMA) is caused by mutations of the survival of motor neuron (*SMN1*) gene and deficiency of full-length SMN protein (FL-SMN). All SMA patients retain one or more copies of the *SMN2* gene, but the principal protein product of *SMN2* lacks exon 7 (SMNΔ7) and is unable to compensate for a deficiency of FL-SMN. SMN is known to oligomerize and form a multimeric protein complex; however, the mechanisms regulating stability and degradation of FL-SMN and SMNΔ7 proteins have been largely unexplored. Using pulse-chase analysis, we characterized SMN protein turnover and confirmed that SMN was ubiquitinated and degraded by the ubiquitin proteasome system (UPS). The SMNΔ7 protein had a twofold shorter half-life than FL-SMN in cells despite similar intrinsic rates of turnover by the UPS in a cell-free assay. Mutations that inhibited SMN oligomerization and complex formation reduced the FL-SMN half-life. Furthermore, recruitment of SMN into large macromolecular complexes as well as increased association with several Gemin proteins was regulated in part by protein kinase A. Together, our data indicate that SMN protein stability is modulated by complex formation. Promotion of the SMN complex formation may be an important novel therapeutic strategy for SMA.

Spinal muscular atrophy (SMA) is an autosomal-recessive motor neuron disease, which is the most common severe hereditary disease of infancy and early childhood. SMA results from survival of motor neuron (SMN) protein deficiency. In humans, SMN is encoded by two genes, *SMN1* and *SMN2* (21). SMA is caused by deletions and other mutations of *SMN1* with retention of *SMN2* in variable copy number (6). *SMN1* primarily produces full-length SMN transcript, while *SMN2* is alternatively spliced producing a majority of transcripts lacking exon 7 (26, 32). Nonetheless, increased *SMN2* copy number ameliorates SMA disease severity in a dose-dependent fashion (11, 19, 38). Features of *SMN2* that may explain its ability to partially compensate for loss of *SMN1* are (i) it produces some full-length SMN protein (FL-SMN), and (ii) it produces a splice variant lacking exon 7 (SMNΔ7) that, although highly unstable, may retain function (20).

SMN is a 38-kDa ubiquitously expressed protein that is found in the nucleus and throughout the cytoplasm (23). SMN oligomerizes via domains encoded by exons 2, 6, and 7 (27, 43) and interacts with Gemins 2 to 8 and unrip to form a multimeric complex (2, 17, 24, 37). The best-characterized function of the SMN complex is to assemble small nuclear ribonucleoprotein particles (snRNPs), critical components of the spliceosome. SMN deficiency has recently been associated with reduced levels of small nuclear RNAs (snRNAs) and abnormally spliced transcripts, suggesting that SMA is due to splicing defects (7, 45). However, SMN may also form other types of multiprotein complexes with diverse functions. For example, SMN associates with Gemin 2 and Gemin 3, but not spliceosomal Sm proteins in neuronal processes and growth cones of primary hippocampal motor neurons, suggesting it may have an axon-specific role independent of snRNP biogenesis (44). The fate of monomeric SMN in cells and whether it has an important functional role is unknown.

The SMNΔ7 protein is the principal protein product of the *SMN2* gene. Although abundant SMNΔ7 transcript is present in human tissues and cells, SMNΔ7 protein is essentially undetectable by Western blotting (25, 32, 40). Even in SMA mice transgenically expressing extremely high levels of SMNΔ7 transcript, SMNΔ7 protein is measurable at only low levels (20). The mechanism behind the apparent instability of SMNΔ7 is unknown. It is possible that loss of the 16 amino acids encoded by exon 7 could result in failure of SMNΔ7 to adopt a normal conformation, destabilizing the nascent protein, and targeting it for immediate degradation. Conformational changes could also disrupt critical SMN interactions or modifications that protect it from degradation. Alternatively, the stability of SMNΔ7 could be principally governed by its ability to oligomerize and form complexes. Importantly, when expressed at high levels in SMA mice, SMNΔ7 extends survival, suggesting that SMNΔ7 retains some function. Because of the potential beneficial role of SMNΔ7, clarifying the underlying mechanisms governing its degradation is likely to be of therapeutic value.

Because SMN disease severity correlates with SMN protein levels in humans and mice (11, 19, 22), a major goal of SMA therapeutics development is identify compounds that increase SMN protein levels. Drug treatments that lead to increased SMN expression could be futile without a basic understanding of SMN protein dynamics since the protein may be degraded as quickly as it is synthesized. In the present study, we characterized the turnover of FL-SMN, SMNΔ7, and disease-associated SMN mutants; critical information in understanding the regulation of SMN protein levels. We demonstrate that recruitment of SMN into SMN-Gemin complexes stabilizes the protein and is regulated by the cyclic AMP (cAMP)-dependent kinase, protein kinase A (PKA).

* Corresponding author. Mailing address: Neurogenetics Branch, NIH, Bldg. 35, Rm. 2A1008, Bethesda, MD 20892. Phone: (301) 435-9288. Fax: (301) 480-3365. E-mail: burnettb@ninds.nih.gov.

† Supplemental material for this article may be found at http://mcb.asm.org/.

▽ Published ahead of print on 22 December 2008.

MATERIALS AND METHODS

Plasmids. SMN point mutations E134K, Y272C, and G279V were introduced into a N-terminal myc-epitope-tagged expression plasmid, pCS2-MT-SMN, by site-directed mutagenesis using a QuikChange site-directed mutagenesis kit (Stratagene). A short hairpin RNA (shRNA)-resistant form of myc-SMNΔ7 was generated by introducing silent mutations in the shRNA-targeting region (G863A, C867T, A870T, and T873C) of myc-tagged SMNΔ7 cDNA. Cells were transfected with FUGENE 6 (Roche, Indianapolis, IN) according to the manufacturer's protocol.

Protein extraction and semiquantitative Western blotting. Cells were lysed in 0.1% Nonidet P-40–0.5% sodium deoxycholate and sonicated for 10 s. For experiments studying SMN ubiquitination, the cell lysates were denatured with 1% sodium dodecyl sulfate (SDS) and then renatured with 4.5% Triton X-100 prior to immunoprecipitation with anti-SMN antibody (BD Transduction Laboratories, San Diego, CA). In addition, cell lysis buffer was supplemented with 2.5 μM ubiquitin aldehyde (Boston Biochem, Cambridge, MA) to inhibit deubiquitinating enzymes and 10 μM MG132 (Biomol International, LP, Plymouth Meeting, PA) to block proteasome degradation. Total protein concentrations were determined by using a BCA protein assay kit (Pierce, Rockford, IL) according to the manufacturer's protocol. Protein lysates were separated on 12 or 15% Tris-glycine acrylamide gels and transferred to membranes. The membranes were probed with mouse anti-SMN antibody at 1:3,000 (clone 8; BD Transduction Laboratories), mouse anti-β-actin antibody at 1:10,000 (Sigma-Aldrich, St. Louis, MO), anti-Gemin 3 antibody at 1:1,000 (12H12; Sigma-Aldrich), anti-Gemin 5 at 1:500 (Abcam, Inc., Cambridge, MA), anti-Gemin 6 at 1:500 (Abcam), anti-Gemin 2 antibody at 1:1,000 (2E17; Abcam), anti-myc at 1:1,000 (Sigma-Aldrich), and antiubiquitin at 1:1,000 (FK2; Biomol International). Quantitative immunoblotting was performed as suggested by the manufacturer (Li-Cor, Lincoln, NE). The membranes were scanned on an Odyssey infrared imaging system (Li-Cor), and the intensity of the protein bands were analyzed by using software provided by the manufacturer. SMN and actin were visualized with a peroxidase-linked goat anti-mouse immunoglobulin G (IgG) secondary antibody at 1:10,000 (Jackson Immuno Labs, Inc., West Grove, PA) and chemiluminescence detection (Perkin-Elmer Life Sciences, Oak Brook, IL). Densitometry of the resulting bands was done by using NIH Image software, and SMN protein amounts were corrected based on actin values.

Cell culture and drug treatment. The human fibroblast cell line from a 3-year-old type I SMA patient with two copies of *SMN2* (GM03813; Coriell Cell Repository, Camden, NJ) was maintained as previously described (39). HEK293T cells were maintained in Dulbecco modified Eagle medium supplemented with 2 mM glutamine, 10% fetal bovine serum, and 1% penicillin-streptomycin (100 U/ml) in an atmosphere of 5% CO_2 and 37°C. For drug treatments, cells were plated and treated 24 h later with 10 μM MG132 (Biomol International), 5 mM Calpeptin (Biomol International), 10 mM ammonium chloride, 1 μM myristoylated PKI, or vehicle for the designated times. The cells were then harvested for RNA or protein isolation and quantified as previously described (39). The average value of untreated cells was normalized to 1.

shRNA knockdown of endogenous SMN. HEK293T cells were successfully transfected with four predesigned SMN shRNA vectors or scrambled vector (SureSilencing; SuperArray, Frederick, MD) according to the manufacturer's instructions. Silencing of SMN expression was confirmed by reverse transcription-PCR analysis and immunoblotting. The shRNA plasmid (insert 5′-AAGG TGCTCACATTCCTTAAATT-3′) showed the highest level of SMN knockdown and was chosen for subsequent experiments.

Pulse-chase protein labeling. Pulse-chase analysis was performed as previously described (34). In brief, HEK293T cells were incubated in cysteine-methionine-free medium (Sigma-Aldrich) for 2 h or 12 h followed by incubation in cysteine-methionine-free medium containing 100 μCi of ^{35}S-labeled cysteine-methionine (GE Healthcare, Piscataway, NJ) for 1 h. After labeling, the cells were washed once with culture medium containing 10-fold excess of unlabeled methionine and cysteine (5 mM each) and then incubated further in the same medium. Cells were collected at the indicated time points and processed for immunoprecipitation with anti-SMN antibody (BD Transduction Laboratories), anti-Gemin 3 antibody (Sigma-Aldrich), anti-Gemin 5 (Abcam), and anti-Gemin 6 antibody (Abcam). Immunoprecipitations were carried out for 6 h at 4°C with antibodies bound to protein G–Sepharose (Sigma-Aldrich). After three washes with lysis buffer (100 mM NaCl, 10 mM Tris-HCl [pH 7.4], 2.5 mM $MgCl_2$, 0.1% NP-40, and protease [Roche]) and phosphatase inhibitor cocktails (Sigma-Aldrich), bound proteins were eluted by boiling in SDS–PAGE sample buffer. Immunocomplexes were separated on SDS–10% PAGE. Gels were dried and exposed to a phosphorimager screen, and the signal visualized with a Storm phosphorimager system (Molecular Dynamics, Piscataway, NJ). Densitometric analysis of protein bands was carried out using ImageQuant PhosphorImager software (Molecular Dynamics).

Ubiquitin proteasome degradation assays. Purified glutathione *S*-transferase (GST)-SMN and GST-SMNΔ7 were iodinated with $Na^{125}I$ by using IodoBeads (Pierce) to a specific activity of 0.25 mCi/mg of protein. ^{125}I-GST-SMN (100,000 cpm) was incubated at 30°C for 6 h in a total volume of 40 μl of reaction mixture containing 50 mM HEPES (pH 7.5); 4 mM ATP; 5 mM $MgCl_2$; 40 mM KCl; 1 mM dithiothreitol (DTT); an energy-regenerating system (10 μg of creatine kinase/ml, 5 mM creatine phosphate, 4 mM GTP); 20 μg of ubiquitin conjugation enzyme fraction (Boston Biochem); 1 μg of ubiquitin aldehyde (Sigma-Aldrich); 4 μg of ubiquitin (Sigma-Aldrich); and 2.5 μg of GST, GST-SMN, or GST-SMNΔ7. Reactions were stopped by adding SDS sample buffer, boiled for 5 min, and resolved on 12% SDS-polyacrylamide gel electrophoresis (PAGE) gels. Phosphorimager analysis was used for quantification.

Equal amounts of ubiquitinated ^{125}I-GST-SMN and ^{125}I-GST-SMNΔ7 were incubated with 5 nM purified 26S proteasome (Biomol, Plymouth Meeting, PA) for 30 min at 37°C in the presence or absence of MG132. ^{125}I-GST-SMN and ^{125}I-GST-SMNΔ7 were precipitated at the designated times on ice with 100 μl of 10% trichloroacetic acid (TCA), and the amount of TCA-soluble protein fragments in the supernatant was quantified by using a gamma counter.

Sucrose gradient centrifugation. Cell extracts were prepared in cell lysis buffer. For sucrose gradient centrifugation experiments, cell extracts were centrifuged on 10 ml of 10 to 30% sucrose gradients in lysis buffer for 4 h at 38,000 rpm in a Sorvall Discovery 90 ultracentrifuge at 4°C. The fractions were then pooled by threes. Immunoprecipitations were carried out as described above. For experiments involving incorporation of radioactive material, proteins were resolved by SDS–12% PAGE, and the gels were subsequently dried and exposed to a phosphorimager screen as described above.

Protein purification. All of the GST fusion proteins were expressed from the GST expression vector pGEX-5X (GE Healthcare) in *Escherichia coli* strain BL21(DE3)/pLysS and purified by using glutathione-Sepharose according to the manufacturer's protocol (GE Healthcare).

In vitro PKA phosphorylation. Purified GST-SMN (1 μg) was incubated with the catalytic subunit of PKA (1 U) for 2 h at room temperature in a buffer (300 μl) containing 50 mM Tris (pH 7.5), 1 mM EDTA, 10 mM $MgCl_2$, 200 mM NaCl, and 0.2 mM DTT in the presence of 300 μM ATP and [γ-^{32}P]ATP. Phosphorylation was stopped by the addition of excess EDTA (15 mM), and samples were resolved by SDS–12% PAGE. Gels were dried and exposed to a phosphorimager screen as described above.

RNA extraction and quantification. The cells were homogenized in 1 ml of TRIzol reagent (Invitrogen, Carlsbad, CA), and total RNA was isolated and converted to cDNA as previously described (15). Primers to amplify human SMN, hGUS, and the 18S RNA were purchased from Applied Biosystems. Quantitative reverse transcription-PCRs (RT-PCRs) were run in triplicate using the ABI Prism 7900 sequence detector system (Applied Biosystems, Foster City, CA). The level of each transcript was quantified by the ddCt method using hGUS or 18S as an endogenous control. The average value of the untreated cells was normalized to 1.

Statistics. Biochemical data were analyzed by using the GraphPad Prism software package (GraphPad Software, Inc., San Diego, CA) and compared statistically by either *t* tests or one-way analysis of variance followed by the Newman-Keuls multiple comparison post hoc test. To compare differences between the three groups, a nonparametric equality of medians test was performed, since the data were not normally distributed. If this was statistically significant, then a pairwise comparison between the two treatment groups was performed using a Mann-Whitney test.

RESULTS

SMN is degraded by the proteasome. Intracellular proteins can be degraded or cleaved by several different proteolytic systems including the UPS, the calcium-activated neutral protease (calpain) system, lysosomal proteases, and autophagy. To better define which systems contribute to SMN degradation, we treated SMA patient-derived fibroblast with the proteasome inhibitor MG132, the cell-permeable calpain inhibitor calpeptin, the lysosome inhibitor ammonium chloride (NH_4Cl), and the autophagy inhibitor 3-methyladenine (3-MA). We found that cells treated with MG132 for 8 h had a >2-fold increase in SMN protein levels, whereas treatment with calpeptin, ammonium chloride, and

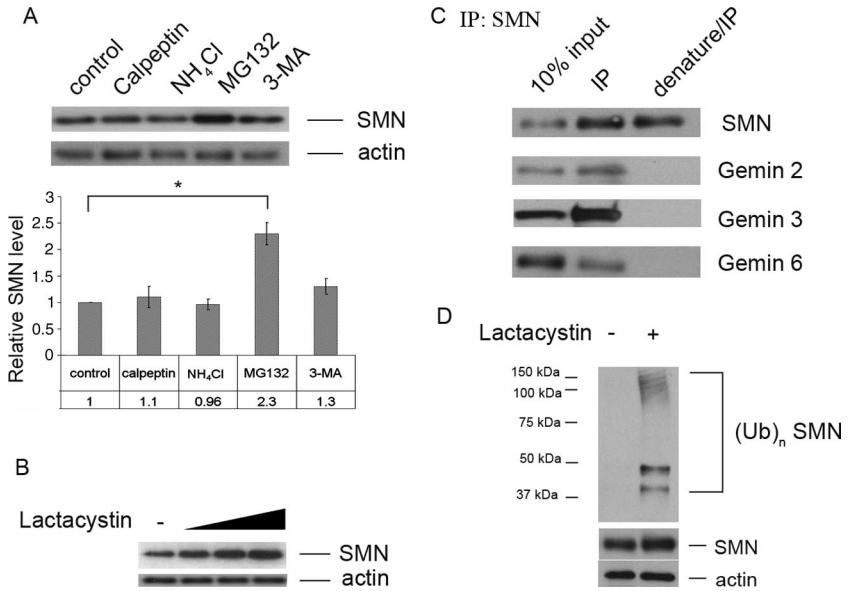

FIG. 1. SMN is ubiquitinated and degraded by the UPS. (A) Treatment of 3813 SMA patient-derived fibroblast with the proteasome inhibitor, MG132 (10 μM); the cell-permeable calpain inhibitor, Calpeptin; the lysosome inhibitor, ammonium chloride (NH_4Cl); and an autophagy inhibitor, 3-MA. Quantification is shown in lower panel. (B) 3813 cells treated with 1, 5, or 10 μM concentrations of the proteasome inhibitor lactacystin. The data represent mean ± the standard error of the mean (SEM) of five independent experiments. *, $P < 0.05$. (C) Cell lysates were denatured with 1% SDS and then renatured with 4.5% Triton X-100 prior to immunoprecipitation with anti-SMN antibody. In addition, cell lysis buffer was supplemented with 2.5 μM ubiquitin aldehyde to inhibit deubiquitinating enzymes. Western bots were probed with antibodies to SMN, Gemin 2, Gemin 3, and Gemin 6. (D) Western blot probed with an antibody to ubiquitin after immunoprecipitation of SMN from cells in the presence or absence of 10 μM lactacystin.

3-MA had no effect on SMN protein levels (Fig. 1A). We also observed a dose-dependent increase in SMN levels using a more specific inhibitor of the proteasome, lactacystin (Fig. 1B). Given the recent report that oxidative stress can increase cross-linking of SMN through intermolecular disulfide bonds (42), we measured the production of reactive oxygen species after treatment with MG132. ROS was unchanged over the treatment time course, indicating that the increased levels of SMN was likely due to proteasome inhibition rather than off-target effects of the drug (see Fig. S1 in the supplemental material).

To further characterize SMN degradation, we examined whether SMN is ubiquitinated prior to degradation. HEK293T cells were incubated with or without lactacystin to induce a buildup of ubiquitinated proteins. Cells were then lysed in nondenaturing lysis buffer containing ubiquitin aldehyde to inhibit deubiquitination and immunoprecipitated with an antibody to SMN. To ensure that the high-molecular-weight ubiquitin positive bands on a Western blot were ubiquitinated SMN and not ubiquitinated proteins that associated with SMN, we disassociated SMN from its binding partners prior to immunoprecipitation by denaturing them with 1% SDS, followed by renaturation in 4.5% Triton X-100. These conditions were sufficient to dissociate SMN from binding partners that have previously been shown to bind SMN even in the presence of high salt (33) (Fig. 1C). Immunoblots of immunoprecipitated proteins were probed with antiubiquitin antibody, and we consistently observed the accumulation of high-molecular-weight ubiquitin-positive bands that represent ubiquitinated forms of the SMN protein (Fig. 1D).

We next investigated whether SMN degradation was altered by ubiquitination. First, we performed in vitro ubiquitination assays using purified GST, GST-SMN, or GST-SMNΔ7 and confirmed SMN ubiquitination by detection of discrete higher-molecular-weight forms of SMN (see Fig. S2 in the supplemental material). GST alone was not ubiquitinated, and assays performed in the absence of ubiquitin showed no high-molecular-weight species. To facilitate degradation, purified 26S proteasome was then incubated with the ubiquitination reaction products for 30 min. Ubiquitination of GST-SMN resulted in a 17-fold increase in the amount of SMN degraded (TCA-soluble radioactive protein fragments) compared to SMN that was not ubiquitinated (Fig. 2A). Similar results were obtained with SMNΔ7, indicating that both FL-SMN and SMNΔ7 were more efficiently degraded once ubiquitinated (Fig. 2A). Of note, we observed no difference in the rate of degradation of ubiquitinated GST-SMN and GST-SMNΔ7 over the indicated time period (Fig. 2B). These data confirm a previous report that SMN is a substrate of the UPS (4). They further indicate that FL-SMN and SMNΔ7 are similarly ubiquitinated and degraded by the proteasome in an in vitro system. Together, these data suggest that factors such as binding partners and posttranslational modification may modulate FL-SMN and SMNΔ7 degradation in vivo.

SMNΔ7 is degraded twice as fast as FL-SMN in cultured cells. The stability of FL-SMN compared to SMNΔ7, the predominant *SMN2* gene product, has been previously investigated by examining SMN turnover in cells after inhibition of protein synthesis using cycloheximide (25, 40). Unfortunately, interpretation of such experiments is confounded by the fact that cycloheximide affects numerous proteins, including potential proteases involved in SMN degradation. In order to more accurately characterize SMN protein turnover, we performed

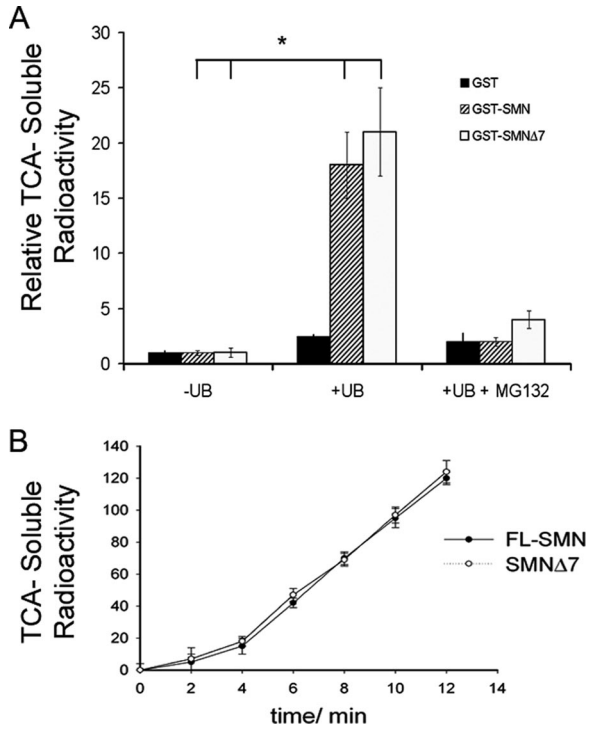

FIG. 2. FL-SMN and SMNΔ7 are ubiquitinated and degraded by the proteasome. (A) Quantification of TCA-soluble SMN fragments after incubation of ubiquitinated or nonubiquitinated ^{125}I-GST-FL-SMN with 5 nM 26S proteasome after 30 min. The data represent mean ± the SEM of three independent experiments. *, $P < 0.05$. (B) Rate of degradation of ubiquitinated ^{125}I-GST-SMN and ^{125}I-GST-SMNΔ7 after incubation with 5 nM purified 26S proteasome and precipitation, at the designated times, on ice with 10% TCA. The data represent mean ± the SEM of three independent experiments.

pulse-chase experiments in cells expressing FL-SMN and SMNΔ7. The advantage of this assay is that newly synthesized proteins are radiolabeled and quantitatively immunoprecipitated at several subsequent time points to determine protein half-life. Because an antibody that distinguishes SMNΔ7 from FL-SMN was not available, we compared the turnover of transiently expressed N-terminal myc-tagged FL-SMN and SMNΔ7. We first verified that the myc-FL-SMN rate of turnover was similar to endogenous SMN (Fig. 3A). Of note, green fluorescent protein (GFP)-SMN was markedly more stable than endogenous SMN and was therefore not useful for analyzing the rate of SMN turnover (Fig. 3A). Using this pulse-chase assay, we determined that the rate of turnover of SMNΔ7 ($t_{1/2}$ = 2.15 h) was on average twofold faster than FL-SMN ($t_{1/2}$ = 4.35 h) (Fig. 3B). Like FL-SMN, SMNΔ7 degradation was unaffected by lysosome, autophagy, and calpain inhibitors (data not shown) but was markedly slowed by the proteasome inhibitor MG132 (Fig. 3C).

Although pulse-chase analysis showed a faster rate of degradation of SMNΔ7 compared to FL-SMN, this difference in the rates of turnover appeared unlikely to fully account for the very low levels of SMNΔ7 protein observed in SMA tissues. Given that SMNΔ7 can associate with FL-SMN (20), we hypothesized that SMNΔ7 is stabilized by its interaction with endogenous FL-SMN. To determine whether the presence of endogenous full-length SMN affected the half-life of SMNΔ7, we knocked down endogenous SMN in the HEK293T cells using shRNAs prior to analyzing SMNΔ7 turnover. We generated a shRNA-resistant form of myc-SMNΔ7 by introducing silent mutations in the shRNA-targeting region in order to target only endogenous SMN and not SMNΔ7. On average, we achieved 90% SMN protein knockdown 72 h after transfection (Fig. 3D). Importantly, reduction of endogenous SMN resulted in further destabilization of SMNΔ7 ($t_{1/2}$ = 0.65 h) (Fig. 3D), indicating that SMNΔ7 degradation is modulated by FL-SMN, presumably through direct interaction.

SMN oligomerization modulates SMN stability. The SMN protein is known to oligomerize and form a large multiprotein complex (35). It has been suggested that incorporation into complex may stabilize SMN, but direct evidence supporting this conclusion has been lacking. Residues encoded by exons 2 and 6 have been demonstrated to be important for SMN self-association (27, 43). In order to define the domains of SMN important for stability, we examined the relative half-life of a panel of SMN deletion mutants transiently expressed in HEK293T cells. We found that deletion of SMN exons 2, 6, and 7 resulted in decreased SMN stability, but deletion of exons 1, 3, 4, and 5 did not. These results support the idea that oligomerization domains are also important for SMN stability (Fig. 4A).

Given the marked reduction in stability observed by deleting exons that mediate SMN self-association, we sought to examine the effects of several disease-causing *SMN1* mutations on SMN protein half-life. We postulated that deletion of exon 7 and the exon 6 missense mutations Y272C and G279V, which lead to disruption of SMN self-association, would reduce SMN half-life, whereas the E134K mutation, which does not affect self-association but reduces interaction with Sm proteins, would not affect SMN half-life (36). To test this hypothesis, we performed pulse-chase analysis using HEK293T cells transiently expressing myc-SMNΔ7, myc-SMN Y272C, myc-SMN G279V, and myc-SMN E134K. We found that the half-lives of SMN G279V ($t_{1/2}$ = 1.5 h) and SMN Y272C ($t_{1/2}$ = 1.25 h) were markedly reduced in comparison to wild-type FL-SMN ($t_{1/2}$ = 4.30 h) (Fig. 4B). In contrast, SMN E134K ($t_{1/2}$ = 4.14 h) had a similar half-life to FL-SMN protein. Together, these data suggest that oligomerization stabilizes SMN and *SMN1* mutations that disrupt SMN self-association increase the rate of SMN degradation.

SMN turnover is reduced by complex formation. To characterize the effect of complex formation on SMN stability, we first compared the half-life of SMN associated with components of the SMN complex to total cellular SMN. We immunoprecipitated Gemin 3, Gemin 5, and Gemin 6, components of the SMN complex, and measured the rate of turnover of the associated SMN (5, 10). Indeed, the fraction of SMN that was associated with Gemin 3, Gemin 5, and Gemin 6 was dramatically more stable compared to total cellular SMN (Fig. 5A). These data indicate that SMN exists in at least two populations: one with a relatively short half-life and another that is resistant to degradation. Since SMN is known to oligomerize and form a large macromolecular complex, it is likely that recruitment of SMN into this complex stabilizes the protein.

Even though we found that SMN was stabilized by association with gemins, it remained unclear whether SMN was in-

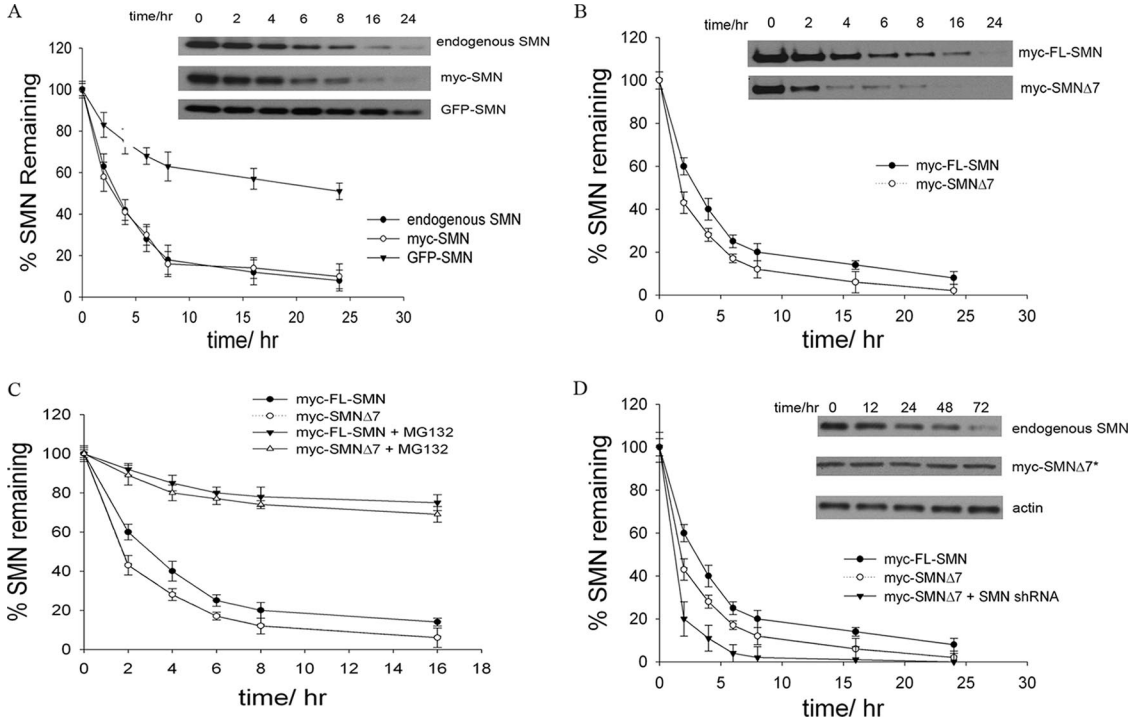

FIG. 3. SMNΔ7 is more rapidly degraded than FL-SMN. (A) Pulse-chase analysis of endogenous SMN, myc-SMN, and GFP-SMN in HEK293T cells. (B) Pulse-chase analysis of myc-SMN and SMNΔ7. (C) Pulse-chase analysis of myc-SMN and SMNΔ7 in the absence or presence of 10 μM MG132. (D) Pulse-chase analysis of SMNΔ7 in HEK293T cells after knockdown of endogenous SMN 72 h after transfection of shRNA targeting SMN. The data represent mean ± the SEM of three independent experiments. Inset shows Western blots of endogenous SMN, the shRNA-resistant myc-SMNΔ7 (designated by an asterisk) and actin at various time points after SMN shRNA transfection.

A

Protein	Half-life ($t_{1/2}$)/hr
FL-SMN	4.3 ± 0.23
SMNΔ1	4.5 ± 0.18
SMNΔ2	3.1 ± 0.32
SMNΔ3	4.2 ± 0.19
SMNΔ4	4.4 ± 0.24
SMNΔ5	4.8 ± 0.33
SMNΔ6	2.1 ± 0.16
SMNΔ7	2.2 ± 0.24

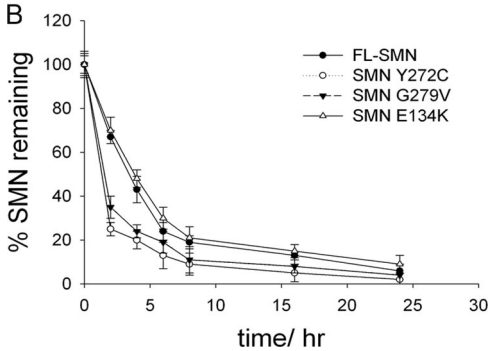

FIG. 4. Residues that are critical for oligomerization modulate SMN stabilization. (A) Pulse-chase analysis of SMN deletion mutants lacking exons 1 through 7. The data represent mean ± the SEM of three experiments. (B) Pulse-chase assay performed on FL-SMN, as well as SMN mutants Y272C and G279V, which show deficits in SMN complex formation, and E134K, which does not affect complex formation. The data represent mean ± the SEM of three experiments.

deed more stable in complex. In order to answer this question, we compared the rate of turnover of SMN that is found in high-molecular-weight complexes to SMN that is found in a monomeric state. We found that if we varied the time we starved our cells of cysteine and methionine prior to pulse-labeling, we could control the proportion of labeled SMN in high-molecular-weight complexes. SMN isolated from HEK 293T cells starved of cysteine-methionine for 2 h, pulse-labeled with radioactive cysteine-methionine, and fractionated by a 10 to 30% sucrose gradient was predominantly found in the low-molecular-weight protein fractions (Fig. 5B). Conversely, SMN was found predominantly in high-molecular-weight fractions after 12 h of starvation. Under these conditions, a similar shift to higher-molecular-weight fractions was observed for Gemin 2, Gemin 3, and Gemin 6, suggesting that SMN and other components of the SMN-Gemin complex were concurrently incorporated into high-molecular-weight complexes (see Fig. S3 in the supplemental material). We compared the stability of SMN monomers to SMN that is mostly in complex by comparing the rate of turnover of SMN in cells starved of cysteine and methionine for 2 and 12 h. The half-life of SMN in cells starved for 12 h ($t_{1/2}$ = 15 h) was >3-fold longer than SMN in cells starved for 2 h ($t_{1/2}$ = 4.28 h) (Fig. 5C). Some of the SMN from cells starved for 12 h were stable for up to 72 h (data not shown). These data further support that SMN exists in at least two populations. One population is only stable for hours, while the other is in large macromolecular complexes and is stable for as long as several days. The half-life of SMN is therefore a function of the abundance of each population.

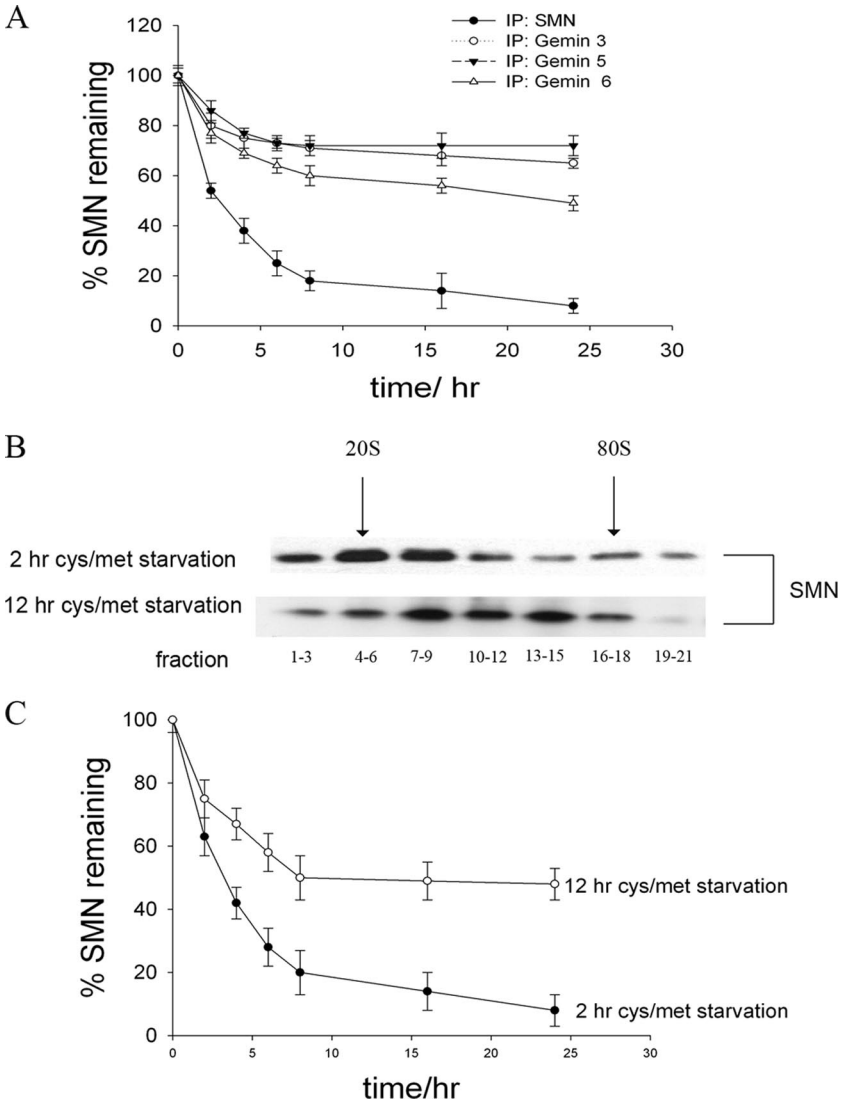

FIG. 5. SMN is stabilized by incorporation into the SMN complex. (A) Pulse-chase assay performed using Gemin 2 and Gemin 3 antibodies to identify SMN that may be in complex. The data represent the means ± the SEM of four experiments. (B) SMN from cells starved of cysteine-methionine for 2 and 12 h and pulse-labeled with radioactive cysteine-methionine, followed by 10 to 30% sucrose gradient separation. (C) Pulse-chase analysis of SMN from cells starved of cysteine-methionine for 2 and 12 h. The data represent mean ± the SEM of five experiments.

PKA increases SMN complex formation and SMN stability. It has been reported that stimulation of cAMP results in increased FL-SMN levels (13, 28). SMN contains three putative PKA phosphorylation sites identified by NetPhos 2.0 server (http://www.cbs.dtu.dk/services/NetPhos) located at threonine 25, threonine 122, and serine 290 (3). We sought to determine whether stimulation of the PKA pathway had posttranscriptional effects on SMN protein levels. Treatment with forskolin, which activates PKA through cAMP, resulted in the accumulation of SMN protein in SMA patient-derived fibroblasts (Fig. 6A and B). Similar results were obtained in HEK293T cells, primary cultures of ventral horn, and primary dorsal root ganglion cells (data not shown). Since forskolin could potentially stimulate *SMN* gene expression, as has been previously reported (28), we examined SMN mRNA levels by quantitative RT-PCR following treatment with forskolin. We detected no significant change in SMN mRNA levels by quantitative RT-PCR (data not shown), suggesting that under these conditions SMN induction by forskolin occurs posttranscriptionally. SMN protein levels were also increased in cells transiently expressing constitutively active PKA (PKA_{ca}), indicating that PKA is a downstream effector of forskolin-induced SMN accumulation (Fig. 6C).

To determine whether SMN may be phosphorylated by PKA, we performed an in vitro phosphorylation assay with the purified catalytic subunit of PKA using purified GST-SMN as the substrate. As expected, SMN was phosphorylated by PKA (Fig. 6D). Mutation of all three potential PKA sites, as well as the previously identified SMN phosphoserines 28 and 31 (9), by site-directed mutagenesis to alanines did not affect PKA phosphorylation of SMN (Fig. 6D and data not shown), suggesting that SMN is potentially phosphorylated by PKA through noncanonical site(s).

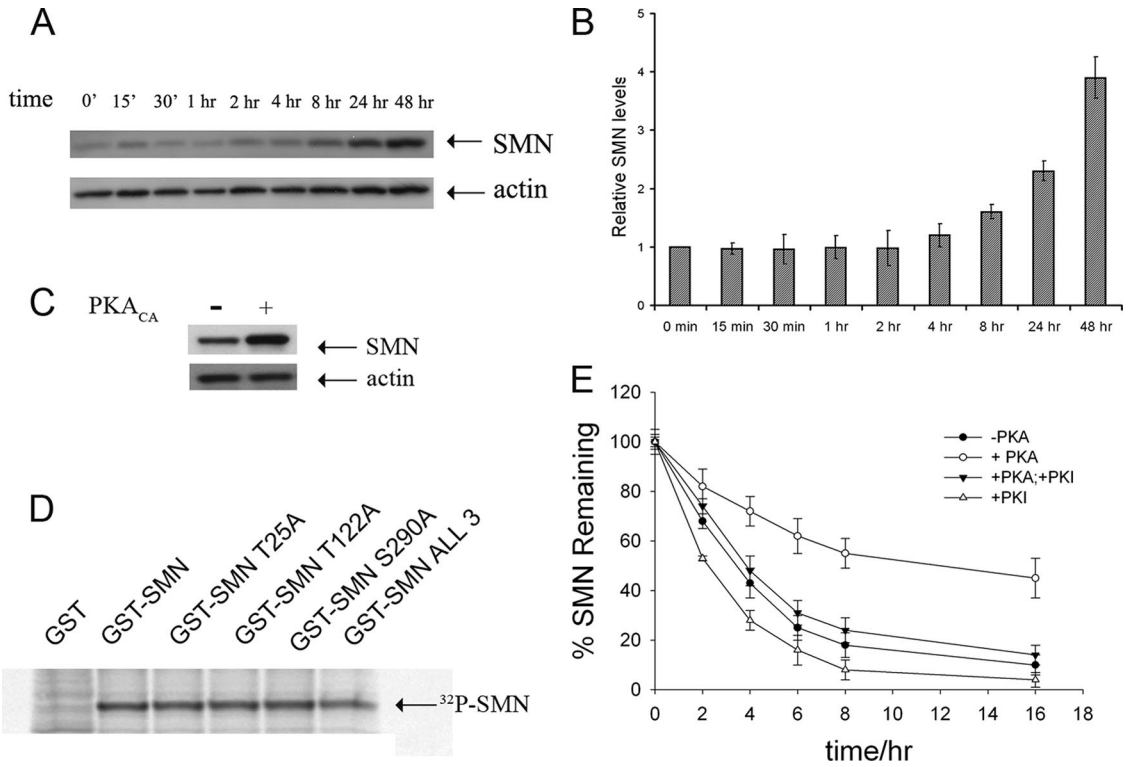

FIG. 6. SMN is stabilized by PKA. (A) Western blot of SMN from 3813 cells treated with forskolin (10 μM) for the indicated times. (B) Quantification of blot in panel A normalized to actin. (C) Western blot of SMN from cells overexpressing constitutively active PKA. (D) Autoradiograph of SMN and point mutants following in vitro PKA assay using purified catalytic subunit of PKA and purified GST-SMN as the substrate. (E) SMN turnover in the presence or absence of constitutively active PKA and the PKA inhibitor PKI.

We next examined whether the observed accumulation of SMN in the presence of PKA is due to inhibition of SMN protein degradation. We analyzed the rate of turnover of SMN in the presence HEK293T cells transiently expressing PKA_{ca} or transfected with a vector control and found that SMN was stabilized in the presence of PKA_{ca} (Fig. 6E). The stabilization of SMN by PKA_{ca} could be partially reversed by treating cells expressing PKA_{ca} with the PKA inhibitor, PKI. In addition, SMN half-life was reduced in cells treated with PKI (Fig. 6E).

To examine whether PKA affects SMN complex formation, we immunoprecipitated SMN from cells expressing either constitutively active PKA or the empty vector and found increased association of SMN with Gemin 5, Gemin 3, and Gemin 2 when normalized to total SMN (Fig. 7A and B). In addition, a greater fraction of SMN was found in the high-molecular-weight fractions obtained by sucrose gradient separation in cells expressing PKA_{ca} compared to cells expressing the vector control, strongly suggesting that PKA inhibits SMN degradation by facilitating incorporation of SMN into high-molecular-weight protein complexes (Fig. 7C).

DISCUSSION

SMA is caused by deficiency of FL-SMN and the failure of SMNΔ7 to compensate for this deficiency. In the present study, we provide evidence that the rate of SMN degradation is principally determined by the ability of SMN to oligomerize and form the SMN-Gemin complex rather than by variable intrinsic rates of degradation of FL-SMN and SMNΔ7. We further show that the rate of SMN degradation can be modified not only by inhibiting the UPS, the endpoint of SMN degradation, but also by stimulation of PKA, which promotes SMN complex formation.

It has long been established that FL-SMN is able to oligomerize and form large multiprotein complexes that are highly chemically stable (35). Our data indicate that in cells FL-SMN exists in at least two populations: a low-molecular-weight population that likely consists of SMN monomers and a high-molecular-weight population that likely consists of complexed SMN. Incorporation of SMN into complexes dramatically shifts its stability from hours to days. In contrast, forms of SMN that lack exons 2, 6, or 7 or SMN mutants, which are known be unable to oligomerize, all decrease the half-life of the SMN protein. It has been observed that although SMNΔ7 poorly self-associates, it can inefficiently interact with FL-SMN in vitro and in cultured cells, presumably by forming heterotypic complexes (20). Our data indicate that SMNΔ7 was more rapidly degraded when endogenous levels of SMN were reduced by siRNA knockdown, suggesting that formation of heterotypic complexes stabilizes SMNΔ7. Importantly, these heterotypic complexes likely retain some function since their presence is associated with extension of survival in SMA mice (20).

Posttranslational modifications may play an important role in determining rates of SMN degradation. It has been previously reported that SMN is phosphorylated at serines 28 and

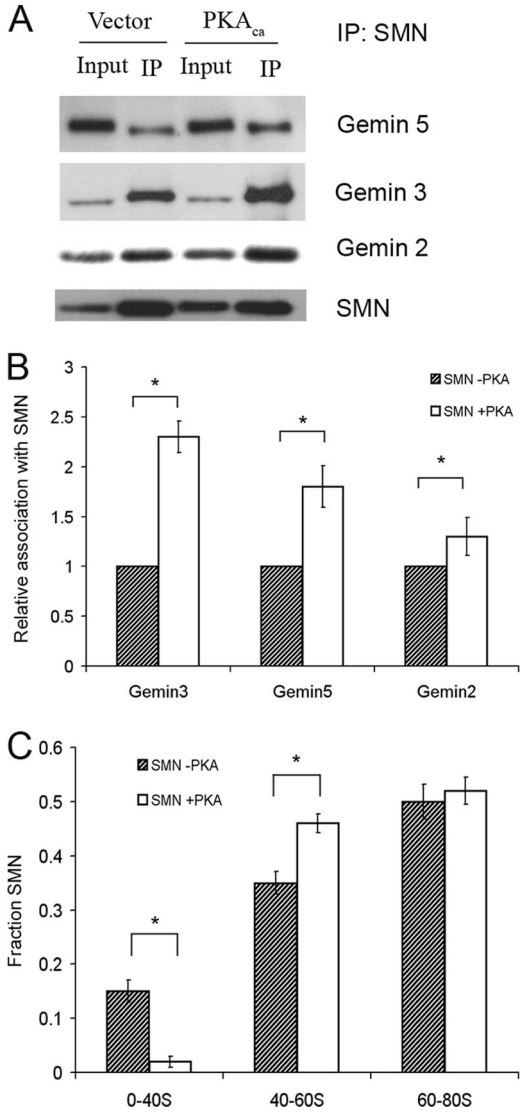

FIG. 7. PKA increases the amount of SMN in complex. (A) Western blot of SMN immunoprecipitated from cells either expressing constitutively active PKA or the empty vector. Blots were probed with antibodies to Gemin 5, Gemin 3, Gemin 2, and SMN. (B) The relative association of gemins with SMN was obtained by normalizing the amount of coimmunoprecipitated Gemin to total SMN protein. Bar graph represents the relative amounts of coimmunoprecipitated Gemin in the presence of PKA to that in the absence of PKA. The data represent mean ± the SEM of three experiments. *, $P < 0.05$. (C) Quantification of SMN in sucrose gradient fractions from cells expressing constitutively active PKA or empty vector. The data represent mean ± the SEM of four experiments. *, $P < 0.05$.

31, and this may regulate snRNP biogenesis (9). Here we show that SMN can be phosphorylated in vitro by PKA and that activation of PKA inhibits SMN degradation in cultured cells. PKA-mediated stabilization of SMN may be due to greater incorporation of SMN into the SMN-Gemin complex, suggesting that SMN protein stability can be manipulated pharmacologically. Identifying compounds that promote SMN complex formation could provide a novel avenue for SMA therapeutics development. One class of compounds that are currently being evaluated in SMA is the β-adrenergic agonists, drugs known to stimulate the cAMP pathway, thus activating PKA (8, 12, 14). β-Adrenergic agonists have been shown to improve muscle strength in human subjects with healthy and diseased muscle (29–31), and daily albuterol treatment had beneficial effects in an open-label pilot study in SMA type II and III patients (16). Salbutamol has been also been shown to increase SMN protein levels in patient-derived fibroblasts (1). Further investigation is needed to determine whether this class of drugs stabilizes SMN via activation of complex formation.

Both FL-SMN and SMNΔ7 are ultimately primarily degraded by the proteasome. We saw no major difference in the rate of degradation of SMN and SMNΔ7 in an in vitro degradation assay, implying that SMNΔ7 is not inherently a better target for degradation by the proteasome. Furthermore, we have not detected alterations in proteasome activity in SMA patient-derived fibroblasts in comparison to age-matched control cell lines using a fluorogenic assay for proteasome activity (unpublished observation), suggesting that there is no overt dysfunction in proteasomal function in SMA patient cells.

Degradation by the proteasome is a highly selective process. The specificity of the UPS is determined by several factors, including posttranslational modifications and recognition by E3 ubiquitin-protein ligases. In most cases, the proteolytic substrates are not recognized in a constitutive manner and must undergo posttranslational modifications such as specific phosphorylation or oxidation that targets them for degradation. The targeting motif can be a single amino acid residue (e.g., the N-terminal residue), a specific sequence (the degron box in cyclins), or a domain (such as a hydrophobic patch) that is not normally exposed. Conversely, protein-protein interactions may sterically hinder access to or recognition of a targeting motif. Increased understanding of the processes and identification of the key regulatory proteins involved in the degradation of SMN could lead to the development of specific antagonists of these molecules (18). Nonetheless, we cannot rule out the possibility that other degradative enzymes may also play a role in SMN turnover.

In the present study, we show that SMN protein stability is highly influenced by oligomerization and complex formation. Missense mutations of SMN that impair oligomerization lead to rapid degradation of SMN, and this may explain why these specific mutations cause severe clinical forms of SMA. We verified that SMN is ubiquitinated and degraded through the UPS. Importantly, the stability of SMN is increased with inhibition of the UPS but also by activation of PKA, which may activate SMN complex formation. While this manuscript was in preparation, it was reported that SMN is cleaved by calpains (41). We did not detect increased steady-state levels of SMN in cells treated with a calpain inhibitor; however, it is possible that SMN degradation pathways are cell type dependent and are differentially regulated in different cell compartments. Further experiments will be required to examine these possibilities. Regardless, these observations indicate that understanding SMN degradation may provide novel avenues for SMA therapeutics development.

ACKNOWLEDGMENTS

We thank George G. Harmison for expert technical assistance. We thank Liu Yang (University of Arkansas) for the myc-tagged FL-SMN

and deletion mutant cDNAs. We thank Peter Wadeson for primary dorsal root ganglion cells.

This study was supported by intramural National Institute of Neurological Disorders and Stroke (NINDS) funds. This study was also supported by a NINDS Competitive Postdoctoral Fellowship (to B.G.B.), a NINDS Career Transition Award (K22-NS0048199-01), and Families of Spinal Muscular Atrophy (to C.J.S.).

REFERENCES

1. **Angelozzi, C., F. Borgo, F. D. Tiziano, A. Martella, G. Neri, and C. Brahe.** 2008. Salbutamol increases SMN mRNA and protein levels in spinal muscular atrophy cells. J. Med. Genet. **45:**29–31.
2. **Baccon, J., L. Pellizzoni, J. Rappsilber, M. Mann, and G. Dreyfuss.** 2002. Identification and characterization of Gemin7, a novel component of the survival of motor neuron complex. J. Biol. Chem. **277:**31957–31962.
3. **Blom, N., S. Gammeltoft, and S. Brunak.** 1999. Sequence and structure-based prediction of eukaryotic protein phosphorylation sites. J. Mol. Biol. **294:**1351–1362.
4. **Chang, H. C., W. C. Hung, Y. J. Chuang, and Y. J. Jong.** 2004. Degradation of survival motor neuron (SMN) protein is mediated via the ubiquitin/proteasome pathway. Neurochem. Int. **45:**1107–1112.
5. **Charroux, B., L. Pellizzoni, R. A. Perkinson, A. Shevchenko, M. Mann, and G. Dreyfuss.** 1999. Gemin3: a novel DEAD box protein that interacts with SMN, the spinal muscular atrophy gene product, and is a component of gems. J. Cell Biol. **147:**1181–1194.
6. **Feldkotter, M., V. Schwarzer, R. Wirth, T. F. Wienker, and B. Wirth.** 2002. Quantitative analyses of SMN1 and SMN2 based on real-time LightCycler PCR: fast and highly reliable carrier testing and prediction of severity of spinal muscular atrophy. Am. J. Hum. Genet. **70:**358–368.
7. **Gabanella, F., M. E. Butchbach, L. Saieva, C. Carissimi, A. H. Burghes, and L. Pellizzoni.** 2007. Ribonucleoprotein assembly defects correlate with spinal muscular atrophy severity and preferentially affect a subset of spliceosomal snRNPs. PLoS ONE **2:**e921.
8. **Green, S. A., B. D. Holt, and S. B. Liggett.** 1992. Beta 1- and beta 2-adrenergic receptors display subtype-selective coupling to Gs. Mol. Pharmacol. **41:**889–893.
9. **Grimmler, M., L. Bauer, M. Nousiainen, R. Korner, G. Meister, and U. Fischer.** 2005. Phosphorylation regulates the activity of the SMN complex during assembly of spliceosomal U snRNPs. EMBO Rep. **6:**70–76.
10. **Gubitz, A. K., Z. Mourelatos, L. Abel, J. Rappsilber, M. Mann, and G. Dreyfuss.** 2002. Gemin5, a novel WD repeat protein component of the SMN complex that binds Sm proteins. J. Biol. Chem. **277:**5631–5636.
11. **Hsieh-Li, H. M., J. G. Chang, Y. J. Jong, M. H. Wu, N. M. Wang, C. H. Tsai, and H. Li.** 2000. A mouse model for spinal muscular atrophy. Nat. Genet. **24:**66–70.
12. **Ikezono, K., M. C. Michel, H. R. Zerkowski, J. J. Beckeringh, and O. E. Brodde.** 1987. The role of cyclic AMP in the positive inotropic effect mediated by beta 1- and beta 2-adrenoceptors in isolated human right atrium. Naunyn Schmiedebergs Arch. Pharmacol. **335:**561–566.
13. **Jablonka, S., M. Beck, B. D. Lechner, C. Mayer, and M. Sendtner.** 2007. Defective Ca2+ channel clustering in axon terminals disturbs excitability in motoneurons in spinal muscular atrophy. J. Cell Biol. **179:**139–149.
14. **Kaumann, A. J., and H. Lemoine.** 1987. Beta 2-adrenoceptor-mediated positive inotropic effect of adrenaline in human ventricular myocardium: quantitative discrepancies with binding and adenylate cyclase stimulation. Naunyn Schmiedebergs Arch. Pharmacol. **335:**403–411.
15. **Kernochan, L. E., M. L. Russo, N. S. Woodling, T. N. Huynh, A. M. Avila, K. H. Fischbeck, and C. J. Sumner.** 2005. The role of histone acetylation in SMN gene expression. Hum. Mol. Genet. **14:**1171–1182.
16. **Kinali, M., E. Mercuri, M. Main, F. De Biasia, A. Karatza, R. Higgins, L. M. Banks, A. Y. Manzur, and F. Muntoni.** 2002. Pilot trial of albuterol in spinal muscular atrophy. Neurology **59:**609–610.
17. **Kolb, S. J., A. K. Gubitz, R. F. Olszewski, Jr., E. Ottinger, C. J. Sumner, K. H. Fischbeck, and G. Dreyfuss.** 2006. A novel cell immunoassay to measure survival of motor neurons protein in blood cells. BMC Neurol. **6:**6.
18. **Lakshmanan, M., U. Bughani, S. Duraisamy, M. Diwan, S. Dastidar, and A. Ray.** 2008. Molecular targeting of E3 ligases: a therapeutic approach for cancer. Expert Opin. Ther. Targets **12:**855–870.
19. **Le, T. T., D. D. Coovert, U. R. Monani, G. E. Morris, and A. H. Burghes.** 2000. The survival motor neuron (SMN) protein: effect of exon loss and mutation on protein localization. Neurogenetics **3:**7–16.
20. **Le, T. T., L. T. Pham, M. E. Butchbach, H. L. Zhang, U. R. Monani, D. D. Coovert, T. O. Gavrilina, L. Xing, G. J. Bassell, and A. H. Burghes.** 2005. SMNDelta7, the major product of the centromeric survival motor neuron (SMN2) gene, extends survival in mice with spinal muscular atrophy and associates with full-length SMN. Hum. Mol. Genet. **14:**845–857.
21. **Lefebvre, S., L. Burglen, S. Reboullet, O. Clermont, P. Burlet, L. Viollet, B. Benichou, C. Cruaud, P. Millasseau, M. Zeviani, et al.** 1995. Identification and characterization of a spinal muscular atrophy-determining gene. Cell **80:**155–165.
22. **Lefebvre, S., P. Burlet, Q. Liu, S. Bertrandy, O. Clermont, A. Munnich, G. Dreyfuss, and J. Melki.** 1997. Correlation between severity and SMN protein level in spinal muscular atrophy. Nat. Genet. **16:**265–269.
23. **Liu, Q., and G. Dreyfuss.** 1996. A novel nuclear structure containing the survival of motor neurons protein. EMBO J. **15:**3555–3565.
24. **Liu, Q., U. Fischer, F. Wang, and G. Dreyfuss.** 1997. The spinal muscular atrophy disease gene product, SMN, and its associated protein SIP1 are in a complex with spliceosomal snRNP proteins. Cell **90:**1013–1021.
25. **Lorson, C. L., and E. J. Androphy.** 2000. An exonic enhancer is required for inclusion of an essential exon in the SMA-determining gene SMN. Hum. Mol. Genet. **9:**259–265.
26. **Lorson, C. L., E. Hahnen, E. J. Androphy, and B. Wirth.** 1999. A single nucleotide in the SMN gene regulates splicing and is responsible for spinal muscular atrophy. Proc. Natl. Acad. Sci. USA **96:**6307–6311.
27. **Lorson, C. L., J. Strasswimmer, J. M. Yao, J. D. Baleja, E. Hahnen, B. Wirth, T. Le, A. H. Burghes, and E. J. Androphy.** 1998. SMN oligomerization defect correlates with spinal muscular atrophy severity. Nat. Genet. **19:**63–66.
28. **Majumder, S., S. Varadharaj, K. Ghoshal, U. Monani, A. H. Burghes, and S. T. Jacob.** 2004. Identification of a novel cyclic AMP-response element (CRE-II) and the role of CREB-1 in the cAMP-induced expression of the survival motor neuron (SMN) gene. J. Biol. Chem. **279:**14803–14811.
29. **Maltin, C. A., M. I. Delday, G. P. Campbell, and J. E. Hesketh.** 1993. Clenbuterol mimics effects of innervation on myogenic regulatory factor expression. Am. J. Physiol. **265:**E176–E178.
30. **Maltin, C. A., M. I. Delday, J. S. Watson, S. D. Heys, I. M. Nevison, I. K. Ritchie, and P. H. Gibson.** 1993. Clenbuterol, a beta-adrenoceptor agonist, increases relative muscle strength in orthopaedic patients. Clin. Sci. **84:**651–654.
31. **Martineau, L., M. A. Horan, N. J. Rothwell, and R. A. Little.** 1992. Salbutamol, a β_2-adrenoceptor agonist, increases skeletal muscle strength in young men. Clin. Sci. **83:**615–621.
32. **Monani, U. R., C. L. Lorson, D. W. Parsons, T. W. Prior, E. J. Androphy, A. H. Burghes, and J. D. McPherson.** 1999. A single nucleotide difference that alters splicing patterns distinguishes the SMA gene SMN1 from the copy gene SMN2. Hum. Mol. Genet. **8:**1177–1183.
33. **Otter, S., M. Grimmler, N. Neuenkirchen, A. Chari, A. Sickmann, and U. Fischer.** 2007. A comprehensive interaction map of the human survival of motor neuron (SMN) complex. J. Biol. Chem. **282:**5825–5833.
34. **Palazzolo, I., B. G. Burnett, J. E. Young, P. L. Brenne, A. R. La Spada, K. H. Fischbeck, B. W. Howell, and M. Pennuto.** 2007. Akt blocks ligand binding and protects against expanded polyglutamine androgen receptor toxicity. Hum. Mol. Genet. **16:**1593–1603.
35. **Paushkin, S., A. K. Gubitz, S. Massenet, and G. Dreyfuss.** 2002. The SMN complex, an assemblyosome of ribonucleoproteins. Curr. Opin. Cell Biol. **14:**305–312.
36. **Pellizzoni, L., B. Charroux, and G. Dreyfuss.** 1999. SMN mutants of spinal muscular atrophy patients are defective in binding to snRNP proteins. Proc. Natl. Acad. Sci. USA **96:**11167–11172.
37. **Pellizzoni, L., J. Yong, and G. Dreyfuss.** 2002. Essential role for the SMN complex in the specificity of snRNP assembly. Science **298:**1775–1779.
38. **Prior, T. W., K. J. Swoboda, H. D. Scott, and A. Q. Hejmanowski.** 2004. Homozygous SMN1 deletions in unaffected family members and modification of the phenotype by SMN2. Am. J. Med. Genet. A **130:**307–310.
39. **Sumner, C. J., T. N. Huynh, J. A. Markowitz, J. S. Perhac, B. Hill, D. D. Coovert, K. Schussler, X. Chen, J. Jarecki, A. H. Burghes, J. P. Taylor, and K. H. Fischbeck.** 2003. Valproic acid increases SMN levels in spinal muscular atrophy patient cells. Ann. Neurol. **54:**647–654.
40. **Vitte, J., C. Fassier, F. D. Tiziano, C. Dalard, S. Soave, N. Roblot, C. Brahe, P. Saugier-Veber, J. P. Bonnefont, and J. Melki.** 2007. Refined characterization of the expression and stability of the SMN gene products. Am. J. Pathol. **171:**1269–1280.
41. **Walker, M. P., T. K. Rajendra, L. Saieva, J. L. Fuentes, L. Pellizzoni, and A. G. Matera.** 2008. SMN complex localizes to the sarcomeric Z-disc and is a proteolytic target of calpain. Hum. Mol. Genet. **17:**3399–3410.
42. **Wan, L., E. Ottinger, S. Cho, and G. Dreyfuss.** 2008. Inactivation of the SMN complex by oxidative stress. Mol. Cell **31:**244–254.
43. **Young, P. J., N. T. Man, C. L. Lorson, T. T. Le, E. J. Androphy, A. H. Burghes, and G. E. Morris.** 2000. The exon 2b region of the spinal muscular atrophy protein, SMN, is involved in self-association and SIP1 binding. Hum. Mol. Genet. **9:**2869–2877.
44. **Zhang, H., L. Xing, W. Rossoll, H. Wichterle, R. H. Singer, and G. J. Bassell.** 2006. Multiprotein complexes of the survival of motor neuron protein SMN with gemins traffic to neuronal processes and growth cones of motor neurons. J. Neurosci. **26:**8622–8632.
45. **Zhang, Z., F. Lotti, K. Dittmar, I. Younis, L. Wan, M. Kasim, and G. Dreyfuss.** 2008. SMN deficiency causes tissue-specific perturbations in the repertoire of snRNAs and widespread defects in splicing. Cell **133:**585–600.